

Microstructure and performance of AZO thin films prepared by sol–gel processing

Rainer Jahn · Peer Löbmann

Received: 18 December 2012 / Accepted: 23 January 2013 / Published online: 5 February 2013
© Springer Science+Business Media New York 2013

Abstract Al-doped zinc oxide (AZO) films were prepared by a wet-chemical coating technique, their microstructure and crystal growth were characterized as a function of the single layer thickness. When similar final thicknesses are attained by more multiple subsequent coating-firing cycles, film porosity is reduced from over 14 to 2 %. Simultaneously the AZO crystallite size is increased from approximately 23 to 60 nm, a preferential c-axis oriented growth is observed. Different substrates (soda-lime glass, soda-lime glass with a SiO₂ barrier coating, borosilicate glass and alkali-free display glass) were used and the resulting AZO films were compared. It is found that the substrate composition primarily affects grain growth and subsequently the electrical performance of the AZO films.

Keywords Thin film · AZO · TCO · Ellipsometric porosimetry · Substrate

1 Introduction

Transparent conducting oxides (TCOs) play a crucial role in display technology and photovoltaics, as electrodes in light emitting diodes and for radiative energy management of architectural glass. Indium-tin oxide (ITO) generally shows outstanding material performance, but alternatives are sought due to the high price and limited availability of In. Among viable substitutes aluminum-doped zinc oxide (AZO) has attracted considerable academic and commercial attention: Its inferior specific resistivity is at least

partially compensated by its lower price. Additionally, surface textures may be induced into AZO films by wet chemical etching that prove highly beneficial for light harvesting in thin film solar cells [1].

Most commercial thin film processing techniques for TCOs are either based on physical or chemical vapor deposition (PVD or CVD). Wet chemical processing, however, provides some specific advantages especially with respect to direct patterning by printing techniques. As the electric performance of sol–gel derived films tends to be 1–2 orders of magnitude inferior to that of materials deposited via the vapor phase, specific process optimization strategies have to be applied. For example the porosity of as-prepared ITO layers can be reduced by a second infiltration step with smaller particles [2]. Another possibility is to assemble films by subsequent coating-firing cycles of thin single layers. As the single layer thickness decreases a larger proportion material freshly deposited is in contact with a preceding crystalline film during thermal treatment. The underlying material then acts as a seed-layer and thus induces homoepitactic crystallization. Additionally, for thin deposits, this heterogeneous nucleation is favored over the homogeneous nucleation within the bulk of the film which would lead to the formation of an undesirable porous polycrystalline network.

The latter interrelationship between single layer thickness and film morphology has already been reported for AZO thin films [3], the authors proposed a zone model for the structure of their TCO films [4, 5]. Recently these observations have been also verified for titania coatings [6].

In this paper the qualitative structural features of AZO coatings as shown in SEM images are backed up by quantitative results obtained from porosity measurements of the respective films by ellipsometric porosimetry (EP). X-ray diffraction experiments (XRD) reveal a distinct preferential c-axis oriented growth of the AZO grains

R. Jahn · P. Löbmann (✉)
Fraunhofer-Institut für Silicatforschung, Neunerplatz 2,
97082 Würzburg, Germany
e-mail: loebmann@isc.fhg.de; peer.loebmann@isc.fraunhofer.de

perpendicular to the substrates surface. In addition to variations of single layer thickness, the effect of the substrate on the film conductivity was investigated. Results indicate that crystallite growth as affected by the different glass substrates used is the determining factor for the final film performance.

2 Experimental procedure

Precursor solutions for coating experiments were prepared by chelating zinc acetate dihydrate with triethanolamine and ethanolamine in a solution of 2-propanol. After heating at 80 °C for 1 h aluminum nitrate nonahydrate was added. The atomic ratio of Zn:Al was set to 1:0.008. All chemicals were purchased from Aldrich and were used without further purification. The viscosity and oxide yield of the sols were adjusted by the amount of 2-propanol in order to facilitate different film thickness with comparable withdrawal rates.

Thin films were prepared on soda-lime glass (Optiwhite, Pilkington NSG) and borosilicate glass (Schott, Borofloat) in the size of $3.3 \times 150 \times 100 \text{ mm}^3$. Additionally soda-lime glasses with a 100 nm SiO_2 barrier coating was prepared by Prinz Optics (Stromberg, Germany), display glass Eagle XP was purchased from Corning.

Thin films were applied by dip coating, the withdrawal rates were varied to adjust single layer thicknesses between 8 and 90 nm, the respective coating-firing cycles were repeated until a final multilayer thickness of 90–125 nm was obtained. The samples were treated in a furnace preheated to 550 °C for 10 min after each coating. Finally, the samples were heated to 500 °C for 1 h in forming gas (95 % Nitrogen and 5 % Hydrogen). For shipping the specimens were sealed under argon atmosphere.

The films with their glass substrates were fractured into about 1 cm^2 pieces and fixed on the SEM sample holders in edged-on manner. Prior to investigation the samples were sputter-coated with Pt to avoid charging. The images were acquired with an in-lens detector at the working distance of 3 mm, by using an accelerating voltage of 5 kV (Field Emission SEM, Ultra 55, Carl Zeiss NTS Inc. Oberkochen, Germany).

Open porosity was determined by atmospheric ellipsometric porosimetry (EP-A), which uses the change of optical characteristics during the water vapor adsorption and desorption, to calculate the open porosity. The ellipsometric results obtained for completely empty pores (n_1) and fully water-filled pores (n_2) were evaluated with Lorentz-Lorenz equation, without requirement of any information on the bulk material. Details regarding these measurements are disclosed elsewhere [7].

Grazing incidence X-ray diffractometry (GIXRD) was performed with a Siemens D-5005 diffractometer (Bruker

AXS GmbH, Karlsruhe, Germany) at an angle of incidence of 0.5°. Crystallite sizes were calculated for individual reflections using the Scherrer-equation. Additionally the median crystallite size was derived by averaging the respective values for the (100), (002), (101), (102) and (110) reflections.

The transmittance of films in the spectral range between 300 and 1,300 nm was determined using a Shimadzu UV-3100 UV–VIS–NIR recording spectrometer combined with a MPC-3100 multi-purpose large sample compartment for UV-3100.

Film resistivities were determined at Fraunhofer IST, Braunschweig, Germany by Hall measurements.

3 Results and discussion

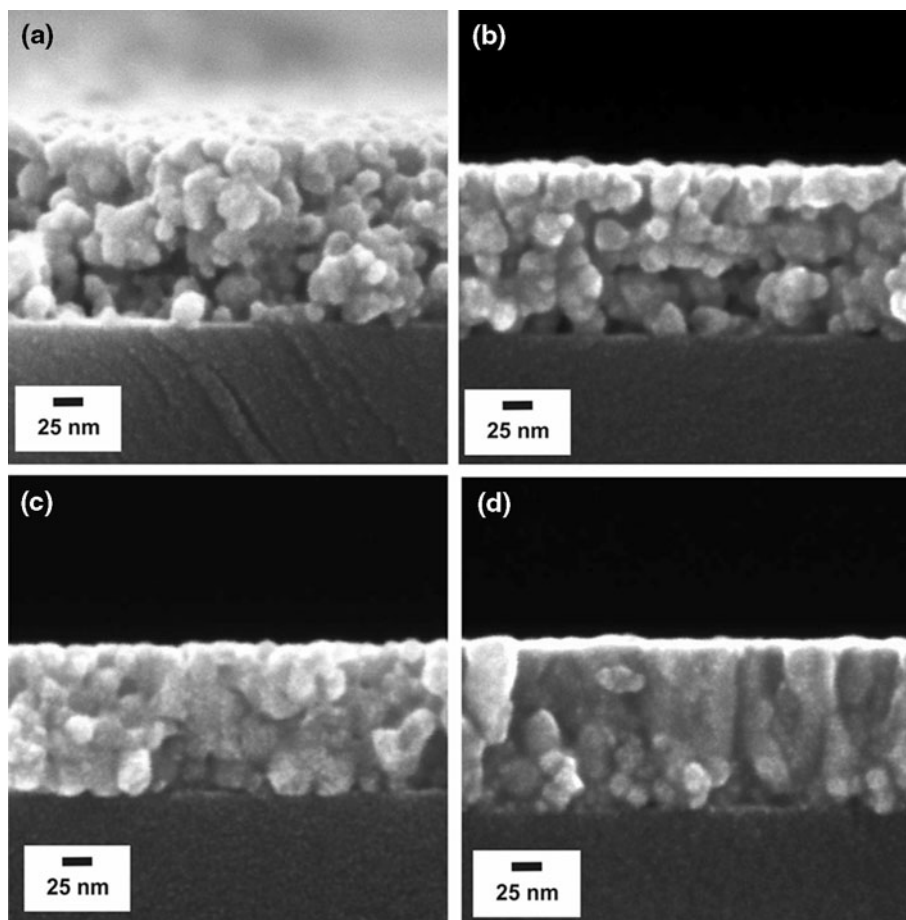
3.1 Effect of multiple coating-firing cycles

Aluminum-doped zinc oxide (AZO) thin films with a final thickness range between 90 and 125 nm were deposited on borosilicate glass (Schott Borofloat) by different numbers of subsequent coating-firing cycles (Fig. 1). In order to achieve the required different single layer thicknesses sol concentration and withdrawal rates were varied respectively. The film prepared by a single deposition (Fig. 1a) exhibits a coarse and porous microstructure. Due to the weak adhesion of these samples to the substrate and weak film cohesion practical handling is difficult. For these samples further characterization by EP as well as the deposition of metallic contact for electric measurements become unreliable.

Films applied by threefold coating show an improved mechanical stability, the SEM image in Fig. 1b implies a layered sequence of three subsequent porous deposits. As the single layer thickness decreases to approximately 16 nm (sevenfold coating-firing) no adjacent boundaries are visible any more (Fig. 1c), the microstructure of this sample appears denser than those of the specimens with higher single layer thicknesses. Nevertheless no distinct layered or columnar features as reported by Schuler et al. [4, 5] can be observed. When the film is prepared by 15 coating-firing cycles (single layer thickness $\sim 8 \text{ nm}$, Fig. 1d) a dense columnar microstructure becomes apparent. Whereas the columns are more distinct near the film surface, the microstructure seems to be rather granular at the substrate-film interface. This observation is consistent with our investigations of Nb-doped TiO_2 films where the columnar microstructure successively evolved within the first deposits [6].

Even though electron microscopy provides valuable qualitative information on the microstructure, the assessment of porosity remains quite vague. In the recent years

Fig. 1 SEM micrographs of AZO films prepared on borosilicate glass by a single coating (a) and 3 (b), 7 (c), 15 (d) subsequent coating-firing cycles



ellipsometric porosimetry (EP) [8, 9] has gained significant importance especially for the characterization of sol-gel derived thin films and multilayer structures [7, 10]. When the ellipsometer is operated under controlled humidity conditions, capillary condensation in pores can be used to determine absolute values for open porosity.

In Fig. 2 water sorption isotherms of the AZO coatings prepared on borosilicate glass are displayed. Whereas the threefold coatings exhibit an open porosity of 14 %, this value is decreased to approximately 4 % when the film consists of seven subsequent coatings. An additional densification is observed if the single layer thickness is further decreased. These findings agree with the qualitative SEM observation (Fig. 1) and provide an additional quantification of the film microstructure.

As outlined before the assembly of sol-gel films by thin multiple coatings goes along with an increase of the respective crystallite size [4, 6]. This general trend is also confirmed by XRD measurements of the AZO films under investigation. However, the (002)/(101) peak ratio for ZnO in random orientation is expected to be 0.44, whereas Fig. 3a reveals a systematic change of this value. As the number of subsequent coatings is increased, the (002) signal becomes more dominant (Fig. 3a) which is

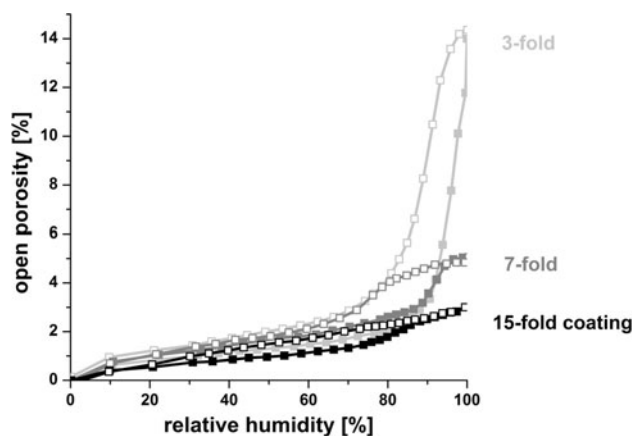


Fig. 2 Water sorption isotherms of AZO thin films prepared by multiple coating-firing cycles as indicated. *Closed and open symbols* denote the adsorption and desorption branch respectively

interpreted as an enhanced occurrence of this crystal plane in the sample. As this plane is perpendicular to the c-axis of the tetragonal unit cell a preferred grain growth takes place in this direction.

This is also reflected in the grain size determination applying the Scherrer equation to different diffraction

Fig. 3 XRD pattern of AZO films prepared with different numbers of coating-firing cycles (a) and crystallite size as determined by applying the Scherrer equation to the (002) and (101) signal (b). Additionally the averaged value from the (100), (002), (101), (102) and (110) peaks are given along with the respective standard deviation

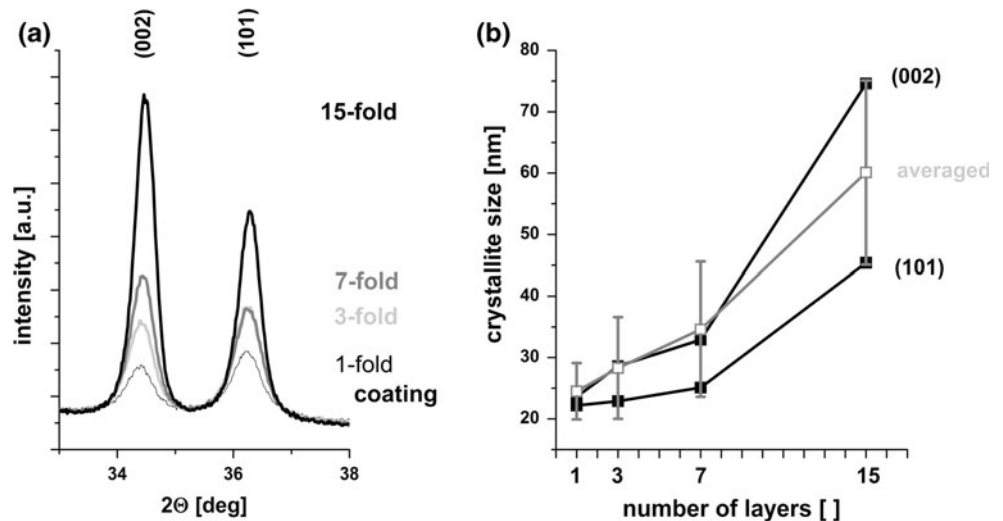


Table 1 Final film thickness, number of single layers and resulting single layer thickness of AZO films prepared on borosilicate glass. Film porosity was measured by ellipsometric porosimetry, crystallite

sizes were calculated from the reflexes indicated according to the Scherrer equation

Total film thickness (nm)	Number of single layers	Single layer thickness (nm)	Open porosity (%)	Crystallite size (nm)		
				Calculated from (002)	Calculated from (101)	(100), (002), (101), (102), (110) Averaged
90	1	90	–	23.6	22.2	24.5 ± 4.6
125	3	42	14	28.6	22.9	28.3 ± 9.3
115	7	16	4	32.9	25.1	34.6 ± 11
120	15	8	2	74.6	45.4	60.1 ± 15

peaks (Fig. 3b): Taking the (002) signal into account the crystallites appear significantly larger than those obtained from the (101) plane. Since no preferential crystal orientation can be induced by the amorphous glass substrate this observation reflects the preferential c-axis oriented columnar growth initiated by the primary coating. In the course of subsequent coating-firing cycles, crystallites with their preferential growth direction perpendicular to the substrate will discriminate other grains with initial alternative orientations [11]. The results so far obtained for AZO coatings on borosilicate glass are compiled in Table 1.

The transmittance of AZO films is displayed in Fig. 4. Samples prepared by threefold and sevenfold coating exhibit a transparency exceeding 75 % in the visible spectral region. For specimens prepared by 15-fold the transmission is reduced below 500 nm. This observation is believed to originate from the adjacent transmittance minimum (whose position can be calculated to about 300 nm) due to optical interference of the quite dense AZO film. For the other more porous coatings with a lower refractive index the minima fall far below the absorption edge of the glass substrate.

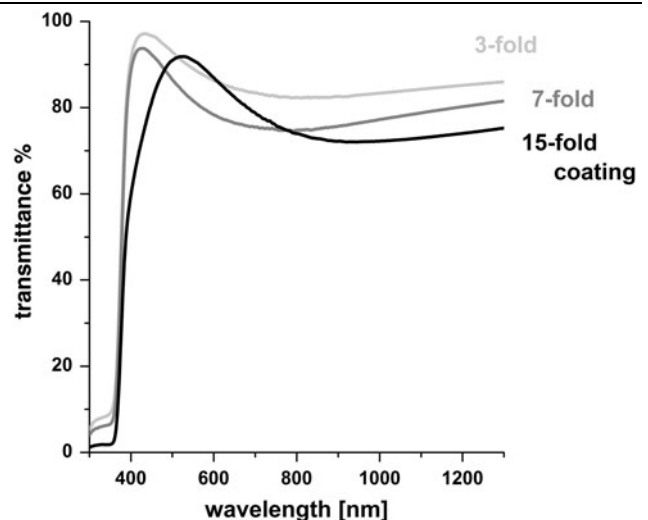


Fig. 4 Transmittance of AZO thin films prepared by multiple coating-firing cycles as indicated

3.2 Effect of substrate materials

The adhesion, performance and long-term stability of functional coatings may be affected by contamination by

constituents of glass substrates. For example the effusion of sodium from soda-lime glass is known to reduce the refractive index of TiO₂ deposited by sol–gel processing [7]. Soda-lime and borosilicate glasses for example provide different sodium contents and for display applications basically sodium-free compositions [12] are available. Alternatively SiO₂ barrier coatings on soda-lime glasses may be applied.

In order to investigate a possible influence of the sodium contents on the performance, AZO films with a final thickness between 90 and 125 nm were deposited by 3-, 7- and 15-subsequent coating-firing cycles. The different substrates used are summarized in Table 2.

The respective sample series did not show any significant differences with respect to their microstructure as characterized by SEM and EP, results corresponding to Figs. 1 and 2 were obtained. The XRD investigations follow the same general trend as observed on borosilicate glass (Fig. 3; Table 1).

In Fig. 5a the specific resistivities of the films are compiled. For each substrate type the conductivity increases when the single layer thickness is reduced i.e. the resulting coating is composed of more thin single layers. This goes

along with the general reduction of porosity as determined by EP. For 15-fold coatings specific resistivities in the range from $2.9 \times 10^{-3} \Omega\text{cm}$ to $4.5 \times 10^{-3} \Omega\text{cm}$ are achieved; there is no systematic difference between the substrates used for these values. For larger single layer thicknesses, systematic variations are observed, however no correlation between electric performance and sodium content is detected: Soda-free display glass exhibits intermediate resistivity for 7- and 15-fold coatings whereas soda lime glass (high sodium content) and borosilicate glass (medium sodium content) show high and low resistivity, respectively. As pointed out above, no microstructural differences are manifested by SEM images and EP measurements.

In Fig. 5b the resistivity of the samples is correlated to their respective crystallite size as determined by applying the Scherrer equation to XRD measurements (averaged value, data not shown). The electric performance of the films is improved as the grain size increases irrespective of the substrate used. It can be concluded that the substrate has an influence primarily on the crystallite growth that downstream governs the electric conductivity. Further studies are aimed at the detailed investigation of the underlying mechanisms.

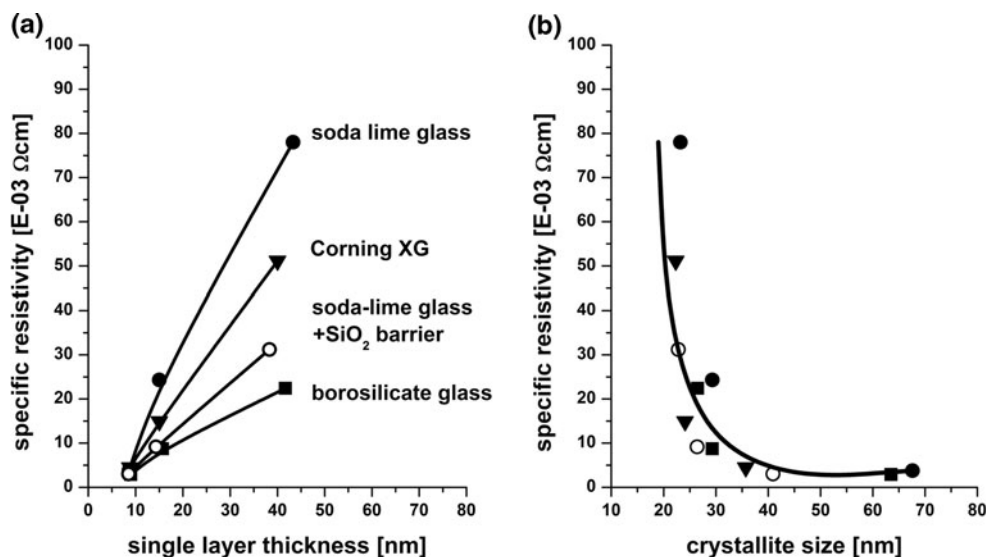
Table 2 Glass substrates used in this study and their respective Na₂O content

Substrate	Trade name	Supplier	Na ₂ O (mass %)
Soda-lime glass	Optiwhite [®]	Pilkington NSG	13
Borosilicate glass	Borofloat [®]	Schott	4
Soda-lime + SiO ₂ barrier	–	Prinz Optics	Barrier
Display glass	Eagle XG	Corning	<0.05

4 Conclusions

The microstructure and porosity of sol–gel derived AZO films can be optimized by choice of the processing parameters i.e. multiple coating techniques. The microstructure of the films as characterized by SEM and EP remains unaltered by the use of different glass substrates. The grain size of the polycrystalline films, however, is identified as the key factor for their electric performance.

Fig. 5 Specific resistivity of AZO films on different substrates as a function of single layer thickness (a) and crystallite size (b). The data markers of (b) correspond to those assigned to the specific substrates in (a)



Acknowledgments The authors are indebted to Angelika Schmitt for the EP measurements. Hall measurements were performed at Fraunhofer IST in Braunschweig, Germany, by Christina Schulz.

References

1. Hüpkes J, Owen J, Pust S, Bunte E (2012) Chemical etching of zinc oxide for thin-film silicon solar cells. *Chem Phys Chem* 13:66–73
2. Prodi-Schwab A, Lüthge T, Jahn R, Herbig B, Löbmann P (2008) Modified procedure for the sol–gel processing of indium-tin oxide (ITO) films. *J Sol-Gel Sci Tech* 47:68
3. Goebbert C, Nonninger R, Aegerter M, Schmidt H (1999) Wet chemical deposition of ATO and ITO coatings using crystalline nanoparticles redispersable in solutions. *Thin Solid Films* 351:79
4. Schuler T, Krajewski T, Grobelsek I, Aegerter M (2004) A microstructural zone model for the morphology of sol-gel coatings. *J Sol-Gel Sci Technol* 31:235
5. Schuler T, Krajewski T, Grobelsek I, Aegerter M (2006) Influence of structure zone model parameters on the electrical properties of ZnO:Al sol–gel coatings. *Thin Solid Films* 502:67
6. Wang C, Meinhardt J, Löbmann P (2010) *J Sol-Gel Sci Technol* 33:148
7. Bittner A, Jahn R, Löbmann P (2011) TiO₂ thin films on soda-lime and borosilicate glass prepared by sol–gel processing: influence of the substrates. *J Sol-Gel Sci Technol* 58:400–406
8. Baklanov MR, Mogilnikov KP, Polovinkin VG, Dultsev FN (2000) Determination of pore size distribution in thin films by ellipsometric porosimetry. *J Vac Sci Technol B* 18(3):1385–1391
9. Baklanov M, Green M, Maex K (2007) Dielectric films for advanced microelectronics. Wiley, West Sussex
10. Bittner A, Schmitt A, Jahn R, Löbmann P (2012) Characterization of stacked sol–gel films: comparison of results derived from scanning electron microscopy, UV–vis spectroscopy and ellipsometric porosimetry. *Thin Solid Films* 520:1880
11. Löbmann P (2012) Transparent conducting oxides. In: Schneller T, Waser R, Kosec M, Payne D (eds) Chemical solution deposition of functional oxide thin films. Springer
12. Bocko E (2008) Highly engineered glass substrates for LCD television: why reducing value is incompatible with consumer expectations. *Inform Disp* 24(5):26